

Thermal properties of bio-flour-filled polyolefin composites with different compatibilizing agent type and content

Hee-Soo Kim^a, Sumin Kim^a, Hyun-Joong Kim^{a,*}, Han-Seung Yang^b

^a Laboratory of Adhesion & Bio-Composites, Program in Environmental Materials Science, Seoul National University, Seoul 151-921, South Korea

^b Wood Materials and Engineering Laboratory, Washington State University, Pullman, WA 99164-1806, USA

Received 30 December 2005; received in revised form 19 September 2006; accepted 20 September 2006

Available online 1 October 2006

Abstract

The main objective of this research was to investigate the effect on thermal properties of the addition of two different compatibilizing agents, maleic anhydride (MA)-grafted polypropylene (MAPP) and MA-grafted polyethylene (MAPE), to bio-flour-filled, Polypropylene (PP) and low-density polyethylene (LDPE) composites. The effect of two different types of MAPE polymer, MA-grafted high-density polyethylene (HDPE-MA) and MA-grafted linear LDPE (LLDPE-MA), was also examined. With increasing MAPP and MAPE content, the thermal stability, storage modulus (E'), $\tan \delta_{\max}$ peak temperature (glass transition temperature: T_g) and loss modulus (E''_{\max}) peak temperature (β relaxation) were slightly increased. The thermal stability, E' and E'' of MAPE-treated composites were not significantly affected by the two different MAPE polymers. The melting temperature (T_m) of the composites was not significantly changed but the crystallinity (X_c) of MAPP- and MAPE-treated composites was slightly increased with increasing MAPP and MAPE content. This enhancement of thermal stability and properties could be attributed to an improvement in the interfacial adhesion and compatibility between the rice husk flour (RHF) and matrix due to the treatment of compatibilizing agent. Attenuated total reflectance (FTIR-ATR) analysis confirmed this result by demonstrating the changed chemical structures of the composites following MAPP and MAPE addition.

© 2006 Elsevier B.V. All rights reserved.

Keywords: Bio-flour; Compatibilizing agent; Interfacial adhesion; Thermal degradation; Viscoelastic properties; Glass transition temperature (T_g); Melting temperature (T_m); Crystallinity (X_c)

1. Introduction

During the last decade, eco-friendly, biodegradable bio-flours and -fibers have been used as reinforcing fillers in the commercial plastic industry to produce composite materials [1–5]. These bio-fillers exhibit a number of attractive advantages, including low cost, low density, low processing requirements, less abrasion during processing, renewability, eco-friendliness and biodegradability [2–4]. However, the main problems of using bio-fillers as a reinforcing filler in the composite system are the low degree of dispersion and poor interfacial adhesion between the hydrophilic bio-filler and the hydrophobic matrix polymer [2,5,6]. This is demonstrated by the difficulty that the polar hydroxyl groups on the surface of the bio-filler have in forming a well bonded interface with a non-polar matrix polymer. This deficiency in

compatibility can lead to a loss in the mechanical and thermal properties of the composites [2,3]. To enhance interfacial adhesion between the bio-filler and matrix polymer, various studies have been conducted by three different treatment methods: surface modification of bio-fillers (chemical treatment), the use of maleic anhydride (MA)-grafted polypropylene (MAPP) [7] and MA-grafted polyethylene (MAPE) [8] as compatibilizing agents and plasma irradiation [9] on bio-fillers (physical pre-treatment). In order to improve the interfacial adhesion of composites, MAPP and MAPE have been widely used as compatibilizing agents through the process of dry blending with the bio-filler and matrix polymer [1,2,7–9].

Thermal analysis (TA) is an analytical experimental technique which measures the thermal properties and interfacial characteristics of a composite material as a function of temperature using a thermal analyzer [3,8,10–12]. To compare the thermal stability of the compatibilizing agent-treated and non-treated composites, the following interfacial characteristics were determined by TA: storage modulus (E'), glass transi-

* Corresponding author. Tel.: +82 2 880 4784; fax: +82 2 873 2318.

E-mail address: hjokim@snu.ac.kr (H.-J. Kim).

Table 1
Chemical constituents of RHF

	Others (%)	Holocellulose (%)	Lignin (%)	Ash (%)	Total (%)
Rice husk flour ^a	5.0	60.8	21.6	12.6	100
Rice husk flour ^b	6.3	59.9	20.6	13.2	100

^a Rice husk, Ref. [16].

^b Specification. From Saron Filler Co.

tion temperature (T_g) and crystallinity (X_c) [10–12]. The higher thermal stability and loss modulus (E'') values of compatibilizing agent-treated composites are due to enhanced interfacial adhesion between matrix polymer and bio-filler, as reported by several authors [8,13,14]. Thermogravimetric analysis (TGA) can measure the moisture content, thermal cleavage, thermal degradation temperature and thermal stability of composite materials [3,8]. Differential scanning calorimetry (DSC) can be used to measure melting temperature (T_m), T_g and crystallization temperature (T_c) of composite materials [7]. Dynamic mechanical thermal analysis (DMTA) has become widely used as a technique for investigating the viscoelastic behavior of composite materials for determining their dynamic modulus such as E' and E'' as a function of temperature [8,12,13].

Polypropylene (PP) and low-density polyethylene (LDPE) are the most important commercial plastics currently used as the matrix polymer in composites due to their relatively superior properties such as high T_m , excellent mechanical/thermal properties, and low density [1,5]. Rice husk flour (RHF) is a surplus byproduct of the rice production process, and is totally biodegradable in the natural environment [2,3]. It therefore shows promise as a bio-filler in composites to replace various materials such as construction materials, furniture and many plastic products in a variety of future industrial applications [6,10].

The purpose of the current research was to investigate the effect of MAPP and MAPE treatment on the thermal properties and interfacial adhesion in the composites. MAPP and MAPE were incorporated over a content range from 0 to 5 wt.% and two different MAPE polymers were used: HDPE-MA and LLDPE-MA. HDPE-MA and LDPE-MA are commercially used in industries requiring enhanced adhesion. Analyses were performed using TGA, DMTA and DSC. We also compared thermal stability and degradation temperature, viscoelastic behavior, T_m , T_g and X_c of the compatibilizing agent-treated (MAPP and MAPE) and non-treated composites. In addition, FTIR-ATR spectra analysis was used to investigate the interfacial bonding and chemical reaction between RHF and matrix polymer in the composites.

2. Experimental

2.1. Materials

PP and LDPE, used as the matrix polymer, were supplied as homopolymer pellets by GS Caltex Corp., South Korea. PP and LDPE had a density of 0.91 and 0.92 g/cm³ and a melt

flow index of 12 and 24 g/10 min, respectively (230 °C/2160 g). The bio-flour used as the reinforcing filler was RHF with a mean particle diameter of 300 μm, obtained from Saron Filler Co. The chemical constituents of RHF are listed in Table 1. MAPP was obtained from Eastman Chemical Products Inc., in the form of Epolene G-3003, which has an acid number of 8 and a molecular weight of 52,300. HDPE-MA and LLDPE-MA were obtained from Crompton Chemical Inc., in the form of Polybond-3009 and Polybond-3109, respectively.

2.2. Compounding and sample preparation

RHF was oven dried at 105 °C for 24 h to adjust the moisture content to 1–3% and then stored in sealed polyethylene bags before compounding. The matrix polymers, PP and LDPE, were blended with the RHF and compatibilizing agents (MAPP and MAPE) altogether in a laboratory-sized, co-rotating, twin screw extruder using three general processes: melt blending, extrusion and pelletizing. The extruder barrel was divided into eight zones with the temperature in each zone being individually adjustable. The temperature of mixing zone in the barrel was maintained at 190 °C (PP) and 160 °C (LDPE) with a screw speed of 250 rpm. The extruded strand was cooled in a water bath and pelletized using a pelletizer. Extruded pellets were oven dried at 80 °C for 24 h and stored in sealed polyethylene bags to avoid unexpected moisture infiltration. To investigate the effect on the thermal properties, composite samples were prepared with 30 wt.% RHF-filler loading and incorporating MAPP and MAPE (1, 3 and 5 wt.%) and the two different MAPE polymers.

2.3. Thermal properties

2.3.1. Thermogravimetric analysis (TGA)

TGA measurements were carried out using a thermogravimetric analyzer (TA instruments, TGA Q500) on 10 mg samples, over a temperature range from 25 to 700 °C, at a heating rate of 20 °C/min. TGA was conducted with the compounds placed in a high quality nitrogen (99.5% nitrogen, 0.5% oxygen content) atmosphere with a flow rate of 20 ml/min in order to avoid unwanted oxidation.

2.3.2. Dynamic mechanical thermal analyzer (DMTA) analysis

To determine their viscoelastic properties, rectangular samples of the composites, 16.0 mm × 6.0 mm × 1.6 mm, underwent DMTA (Rheometric Scientific DMTA IV, NICEM at Seoul National University) examination with the single cantilever method. The RHF-PP and RHF-LDPE composites were

analyzed at the same frequency of 1 Hz and at a strain rate of 0.3% (RHF–PP) and 0.1% (RHF–LDPE). The temperature ranges of RHF–PP and RHF–LDPE composites were -80 to 150 °C and -90 to 120 °C, respectively, at a scanning rate of 5 °C/min. E' , E'' and $\tan \delta$ of the samples were measured as a function of temperature.

2.3.3. Differential scanning calorimetry (DSC) analysis

DSC analysis was carried out using a TA Instrument DSC Q 1000 (NICEEM at Seoul National University) with 5–8 mg of sample. Each sample was scanned from -80 to 200 °C at a heating rate of 10 °C/min and then cooled at the same rate under a nitrogen atmosphere. Thermal properties, such as T_m and T_g , were determined from the second scan. T_m was defined to be the maximum of the endothermic melting peak from the heating second scan and T_g as the deflection of the baseline in the cooling second scan. The specimens' relative degree of X_c was calculated according to the following equation:

$$X_c = \frac{\Delta H_f \times 100}{\Delta H_f^0 w}$$

where ΔH_f is the heat of fusion of the PP, LDPE and composites, ΔH_f^0 the heat of fusion for 100% crystalline PP ($\Delta H_{100} = 138$ J/g) [14] and LDPE ($\Delta H_{100} = 290$ J/g) [15] and w is the mass fraction for PP and LDPE in the composites.

2.4. Attenuated total reflectance (FTIR-ATR) measurements

The infrared spectra in the FTIR-ATR of MAPP, MAPE, composites and compatibilizing agent-treated composites were obtained using a Nexus 870 FTIR spectrophotometer (Thermo Nicolet Instrument Corp. Madison, WI, USA). A diamond was used as an ATR crystal. The samples were analyzed over the range of 525 – 4000 cm^{-1} with a spectrum resolution of 4 cm^{-1} . All spectra were averaged over 32 scans. This analysis of the composites was performed at point-to-point contact with a pressure device.

3. Results and discussion

3.1. Thermogravimetric analysis

Fig. 1 shows the dynamic TGA curves of the PP and RHF-filled PP composites with MAPP content ranging from 0 to 5 wt.%. The PP weight loss occurred in a one-step degradation process from 400 to 500 °C. This result was confirmed by the presence of only one peak in derivative thermogravimetric curve (DTG_{max}) temperature at 480 °C (Table 2). This result confirmed that PP is composed of the carbon–carbon bonds in the main-chain, thereby allowing a temperature increase to promote random scission, with associated thermal degradation and thermal depolymerization occurring at the weak sites of the PP main chains [3,10,16]. Above 500 °C, the quantity of PP residue was very small due to the further breakdown of the PP thermal degradation materials into gaseous products at higher temperature. However, the thermal degradation of RHF-filled PP composites occurred in a two-step degradation process, as also confirmed by

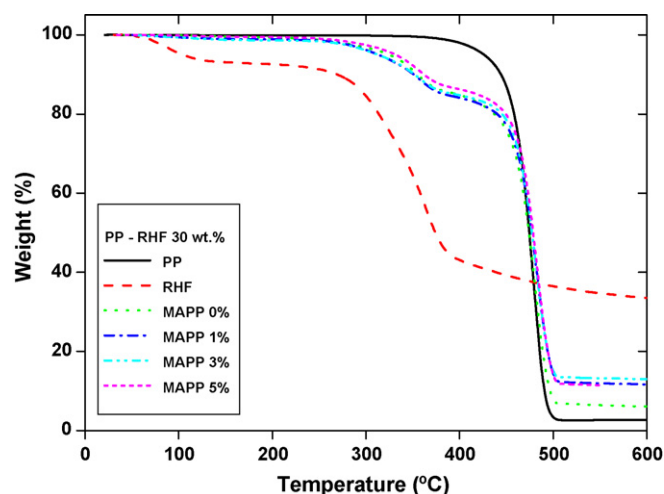


Fig. 1. TGA curves of PP, RHF and RHF-filled PP composites.

*TGA curve of RHF from Ref. [3].

the presence of two peaks for DTG_{max} temperature at 355 and 481 °C (Table 2). In the TGA curves, the first thermal degradation step may have corresponded to the hemicellulose, cellulose and lignin constituents in RHF, after which the second thermal degradation step of PP was observed. This two-step degradation process was further demonstrated in that the thermal degradation temperature of the major constituents in RHF was lower than that of PP, i.e., the depolymerization of hemicellulose mainly between 150 and 350 °C, the random cleavage of the glycosidic linkage of cellulose between 275 and 350 °C, and the degradation of lignin between 250 and 500 °C [16–19]. Above 400 °C, and before the thermal degradation involving the cellulose and hemicellulose cleavage, C–O and C–C bonds are formed from volatile materials such as CO and CH_4 [3].

The TGA curves of the composites according to different MAPP and MAPE (HDPE-MA) contents are shown in Figs. 1 and 2, respectively. The thermal stability and degradation temperature of MAPP- and HDPE-MA-treated composites were slightly higher than those of non-treated composites and were slightly increased with increasing MAPP and HDPE-MA content. The improved thermal stability of the compatibilizing agent-treated composites was due to enhanced interfacial adhesion and additional intermolecular bonding which produces an

Table 2

Summary of DTG_{max} degradation temperature of composites and compatibilizing agent (MAPP and MAPE)-treated composites at different compatibilizing agent contents

Specimens	First peak (°C)	Second peak (°C)
PP	No peak	480.1
PP–RHF 30 wt.%	355.2	481.2
MAPP 1%	360.1	484.2
MAPP 3%	361.5	485.6
MAPP 5%	362.3	486.2
LDPE	No peak	486.1
LDPE–RHF 30 wt.%	355.2	491.8
HDPE-MA 1%	358.7	492.4
HDPE-MA 3%	359.8	494.6
HDPE-MA 5%	361.4	496.5

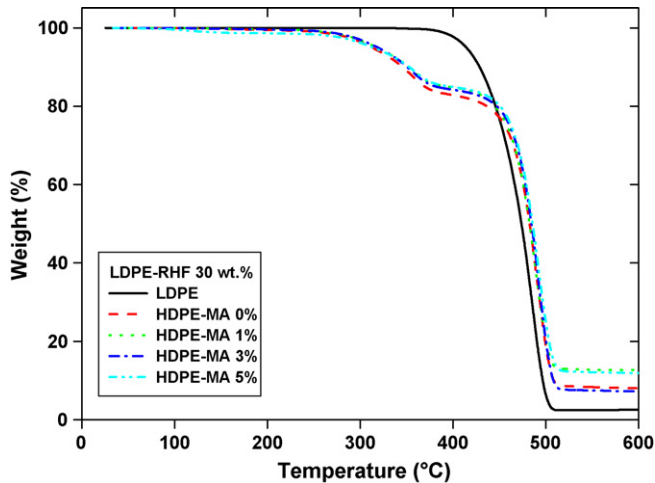


Fig. 2. TGA curves of LDPE and RHF-filled LDPE composites.

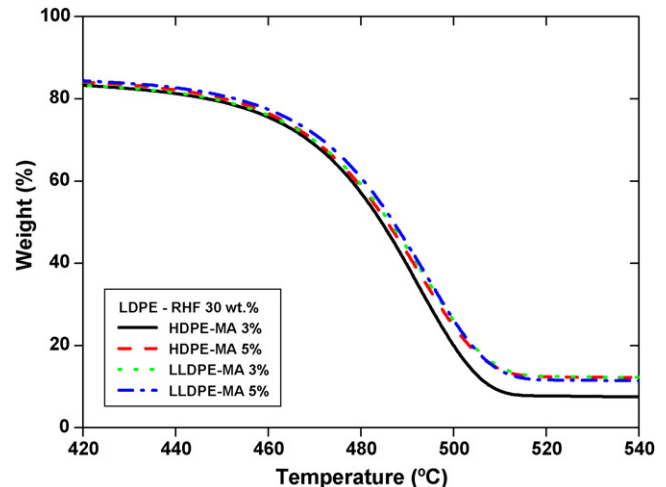


Fig. 4. TGA curves of RHF-filled LDPE composites according to the two different MAPE polymers.

esterification reaction between hydroxyl groups of RHF and the anhydride functional group of MAPP and MAPE [8,19]. Fig. 3 shows the hypothetical structure between hydroxyl groups of RHF and the anhydride functional group of MAPP and MAPE at the interface. The composites with 5% MAPP and HDPE-MA content had the highest thermal stability and this content was therefore chosen as the proper addition to improve the interfacial adhesion of composites. Table 2 shows the first and second DTG_{max} degradation temperature of the composites and compatibilizing agent-treated composites at different compatibilizing agent contents. The first and second DTG_{max} degradation temperature of the composites with MAPP and HDPE-MA was slightly shifted to a higher temperature compared to the non-treated composites and was slightly increased with increasing MAPP and HDPE-MA content. This result indicated that the use of a compatibilizing agent in the composite system improved the thermal stability of the composites [2,6–8]. However, the non-treated MAPP and MAPE composites were easily thermally degraded by increasing temperature due to poor interfacial adhesion between the bio-flour and matrix poly-

mer which degraded the thermal properties of the composites [3].

Fig. 4 presents the TGA curves of RHF-filled LDPE composites according to the two different MAPE polymers. The thermal stability and degradation temperature of the MAPE-treated composites were not affected by the type of MAPE polymers.

3.2. Dynamic mechanical thermal analyzer (DMTA) analysis

Fig. 5 shows the E' of PP and RHF-filled PP composites as a function of temperature. With increasing temperature, the E' values of PP and composites significantly decreased due to the increase polymer chain mobility of the matrix at higher temperatures [3]. The reduction in E' of LDPE and RHF-filled LDPE composites is also shown in Fig. 6. As can be seen in Figs. 4–6, with the incorporation of RHF in PP and LDPE, the E' of PP and LDPE was significantly increased at higher temperature. This is probably due to the increased stiffness of the PP and LDPE with

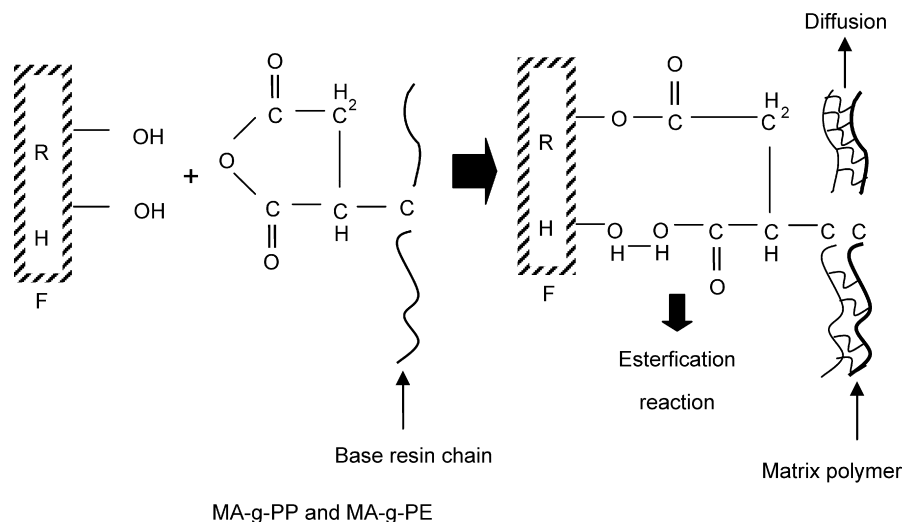


Fig. 3. Hypothetical structure of compatibilizing agent between hydrophilic RHF and hydrophobic matrix polymer [2,7].

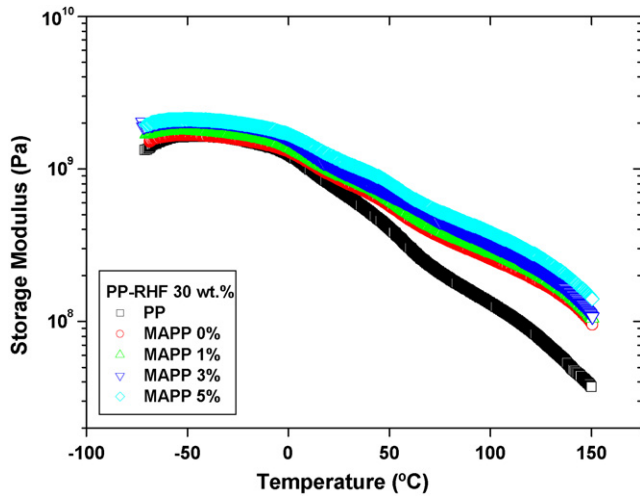


Fig. 5. Storage modulus of PP and RHF-filled PP composites at different MAPP contents.

the reinforcing effect imparted by the RHF which allows for greater stress transfer at the interface from the matrix to the RHF [13]. This result is confirmed by the mechanical properties of natural fiber-reinforced composites. Mohanty et al. [8] reported that the tensile and flexural strengths of jute fiber-reinforced HDPE composites were much higher than those of HDPE. This improved mechanical property of the composites was primarily attributed to the reinforcing effect imparted by the fibers, which allowed a uniform stress distribution from continuous polymer to dispersed fiber phase [8].

The E' of RHF-filled PP and LDPE composites at different MAPP and MAPE content is also seen in Figs. 5 and 6. With increasing MAPP and MAPE content, the E' of composites was slightly increased compared to that of the non-treated composites. The enhanced stiffness of the composites was primarily attributed to the improved compatibility between the RHF and PP, as a result of the enhanced stiffness of the composites [13,14]. The E' value was maximized for the 5% MAPP and MAPE content composites. Fig. 7 presents the E' value of RHF-filled LDPE

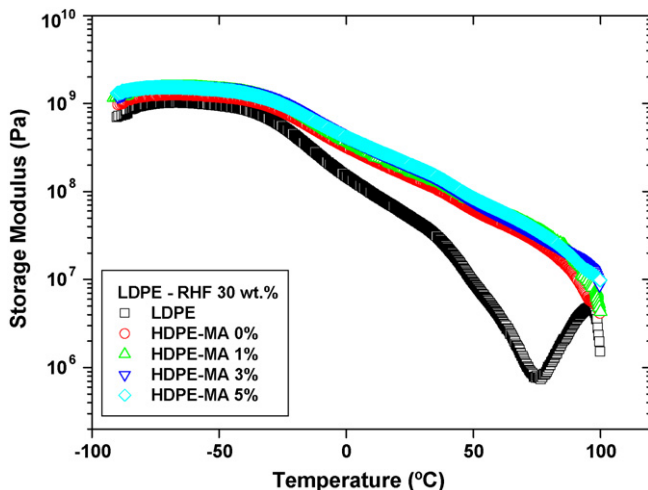


Fig. 6. Variation of storage modulus of LDPE and RHF-filled LDPE composites at different MAPE (HDPE-MA) contents.

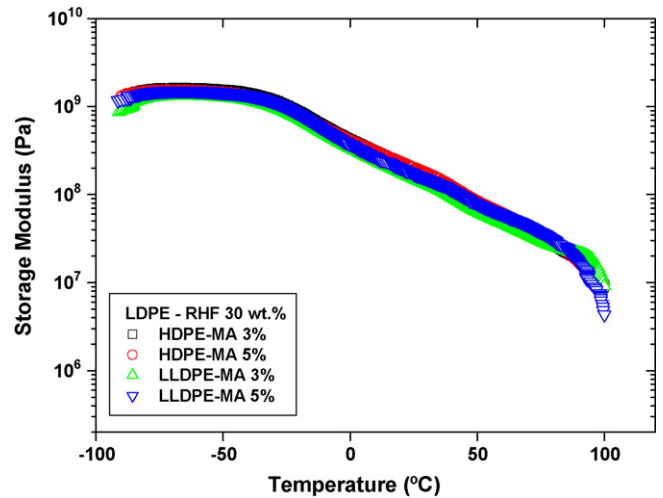


Fig. 7. Variation of storage modulus of RHF-filled LDPE composites according to the two different MAPE polymers.

composites according to the two different MAPE polymers. The stiffness of the MAPE-treated composites was not significantly changed by the two different base resins, indicating that the stiffness of the composites is not affected by the MAPE polymers.

The temperature dependence of $\tan \delta$ for the RHF-filled PP composites at different MAPP contents is presented in Fig. 8. $\tan \delta$ was obtained from the ratio of E'' (viscous phase) to E' (elastic phase). The $\tan \delta_{\max}$ peak can also provide information on the T_g and energy dissipation of composite materials [8,13,20]. With increasing temperature, the $\tan \delta$ values of PP and composites increased due to the increased polymer chain mobility of the matrix. From the $\tan \delta_{\max}$ peak temperature in Table 3, T_g of the composite was slightly shifted to a higher temperature with increasing MAPP content, which may indicate better interfacial interaction between RHF and matrix at the interface [8]. The $\tan \delta$ values of MAPP-treated composites were lower than those of non-treated composites over the complete temperature range, indicating that energy dissipation of the MAPP-treated composites was less than that of non-treated MAPP composites. The $\tan \delta$ values were lowest for the 5% MAPP content

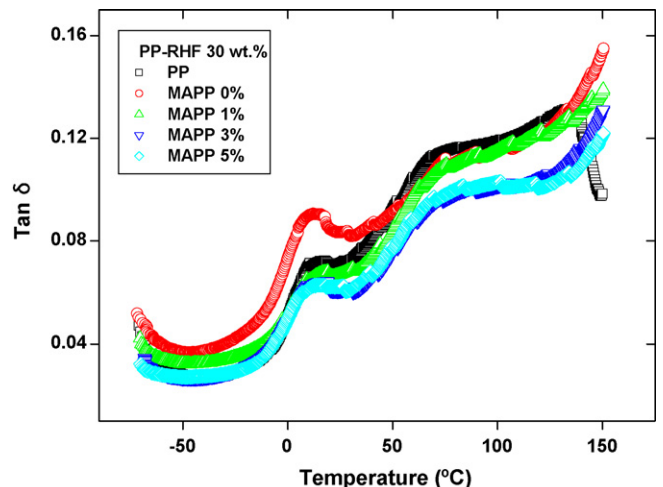


Fig. 8. $\tan \delta$ of PP and RHF-filled PP composites at different MAPP contents.

Table 3

Summary of $\tan \delta_{\max}$ peak and E''_{\max} peak temperature of composites at different compatibilizing agent contents with the two different MAPE polymers

Specimens	$\tan \delta_{\max}$ peak temperature ($^{\circ}\text{C}$)
PP	15.3
PP-RHF 30 wt. %	15.7
MAPP 1%	19.1
MAPP 3%	20.2
MAPP 5%	21.3

Specimens	E''_{\max} temperature ($^{\circ}\text{C}$)
LDPE	-23.9
LDPE-RHF 30 wt. %	-21.7
HDPE-MA 1%	-20.5
HDPE-MA 3%	-19.6
HDPE-MA 5%	-19.4
LLDPE-MA 1%	-21.1
LLDPE-MA 3%	-20.6
LLDPE-MA 5%	-19.7

composites. Energy dissipation may occur by the interface. The improved interfacial bonding of the MAPP-treated composites may be characterized by lower energy dissipation [8]. Therefore, we can conclude that the δ value of the composites is governed by the interfacial adhesion and energy dissipation between the RHF and matrix at the interface.

Fig. 9 shows the variation of the E'' (viscous behavior) of LDPE and RHF-filled LDPE composites at different MAPE contents. We could not measure the T_g of LDPE (-135°C) [21] as it was not sufficiently cooled down to this temperature. However, it is evident that the E''_{\max} peak temperature of LDPE- and MAPE-treated composites was in the range of -23 to -19°C , which may be attributed to β relaxation. The β relaxation temperature of LDPE is related to having properties of the glass–rubber transition and the branched structures of the main chains [22]. However, the β relaxation temperature of HDPE was not observed due to the absence of these branch structures [8]. From the E''_{\max} peak temperature in Table 3, the β relaxation

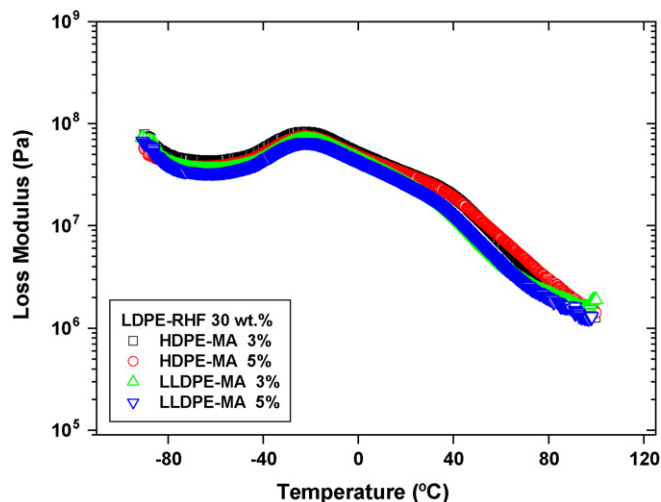


Fig. 10. Variation of loss modulus of RHF-filled LDPE composites according to the two different MAPE polymers.

temperature of the composites was shifted to higher temperature with increasing MAPE content, possibly due to additional bonding between the RHF and LDPE which decreases the polymer chain mobility and thus increases the β relaxation temperature of MAPE-treated composites. Fig. 10 shows the E'' values of RHF-filled LDPE composites according to the two different MAPE polymers. This indicated that the viscous behavior of the composites was not affected by the MAPE polymers.

3.3. Differential scanning calorimetry (DSC) analysis

Fig. 11 presents the second heating thermograms for RHF-filled PP (a) and LDPE (b) composites at different MAPP and MAPE content. The T_m of MAPP- and MAPE-treated composites was obtained from the maximum of the endothermic melting peak. The T_m of composites was not significantly changed by the addition of MAPP and MAPE. Table 4 lists T_g , T_m , ΔH_f and X_c for PP, LDPE, RHF-filled PP and LDPE composites at different compatibilizing contents and with the two different MAPE polymers. The T_g of composites was slightly shifted to a higher temperature with increasing MAPP content. This result was confirmed by $\tan \delta_{\max}$ peak temperature (T_g) of MAPP-treated composites. This may be attributed to the additional bonding between the RHF and PP due to anhydride group of MAPP [2,7]. The DSC and DMTA procedures produced quite different T_g results. The T_g value determined by DSC depended on the thermal history of the sample, whereas that by DMTA was obtained from $\tan \delta$ of the sample, which was itself determined in the experiment whereby the deforming force and oscillating frequency were selected and scanned automatically through a range of values [23].

We could not detect the T_g of LDPE and RHF-filled LDPE composites with different MAPE contents because they were not sufficiently cooled down to T_g (-135°C) of LDPE. However, we can expect that the T_g of MAPE-treated composites may be slightly changed due to the existence of interfacial bonding between the RHF and LDPE at the interface. A slight incre-

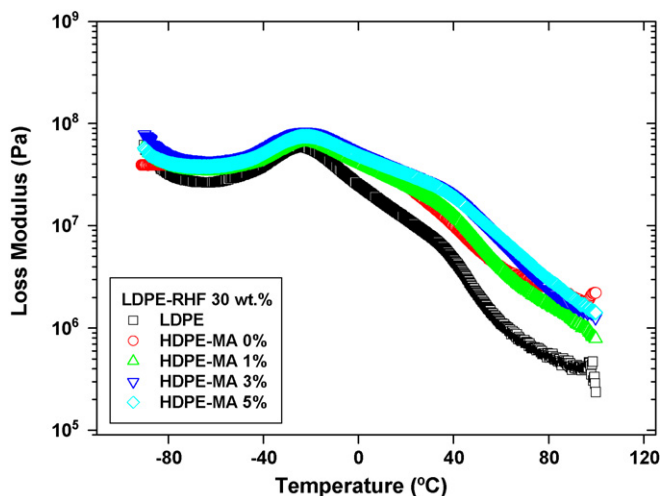


Fig. 9. Variation of loss modulus of LDPE and RHF-filled LDPE composites at different MAPE (HDPE-MA) contents.

Table 4

Summary of T_g , T_m , ΔH_f and X_c for PP, LDPE, RHF-filled PP and LDPE composites at different compatibilizing agent contents with the two different MAPE polymers

	T_g ($^{\circ}\text{C}$)	T_m ($^{\circ}\text{C}$)	ΔH_f (J/g)	Crystallinity degree (%)
PP	-8.4	167.5	80.8	58.5
PP-RHF 30wt.%	-7.9	165.8	59.2	61.2
MAPP 1%	-7.6	164.4	62.9	65.1
MAPP 3%	-6.4	164.0	64.8	67.1
MAPP 5%	-5.1	165.4	65.6	67.9
LDPE	-	103.8	150.1	51.7
LDPE-RHF 30wt.%	-	104.8	102.6	50.5
HDPE-MA 1%	-	103.0	107.7	53.1
HDPE-MA 3%	-	102.8	111.4	54.9
HDPE-MA 5%	-	101.8	115.9	57.1
LLDPE-MA 1%	-	103.7	106.1	52.3
LLDPE-MA 3%	-	103.4	109.1	53.7
LLDPE-MA 5%	-	102.5	111.5	55.9

ment in the X_c of the composites with increasing MAPP and MAPE content can also be observed in Table 4. The improvement in the X_c value of the composites was due to the coupling effect of MAPP and MAPE which extend the predominance of the crystallization process. Table 4 also presents the X_c values

of RHF-filled LDPE composites according to the two different MAPE polymers. The X_c values of composites with HDPE-MA were slightly higher than those of LLDPE-MA composites at all compatibilizer contents, suggesting that the proper method to enhance the interfacial adhesion of composites with LDPE matrix polymer is the treatment of commercially available MAPE with the HDPE-MA compatibilizer.

3.4. FTIR-ATR measurements

Figs. 12 and 13 show the FTIR-ATR spectra of MAPP and HDPE-MA, respectively, compatibilizing agent-treated and non-treated composites. Two special absorbance peaks are evident at 1774 and 1790 cm^{-1} , which were attributed to MA symmetric C=O stretching of MAPP and MAPE, respectively [24,25]. This result suggests that MAPP and MAPE interact with RHF by forming covalent linkage and ester bonding between the MA group of MAPP and MAPE and the hydroxyl groups at the RHF surface [7,8]. This result was clearly confirmed by the two special peaks that are evident at 1740 and 1730 cm^{-1} , respectively, which may have resulted from the esterification of the

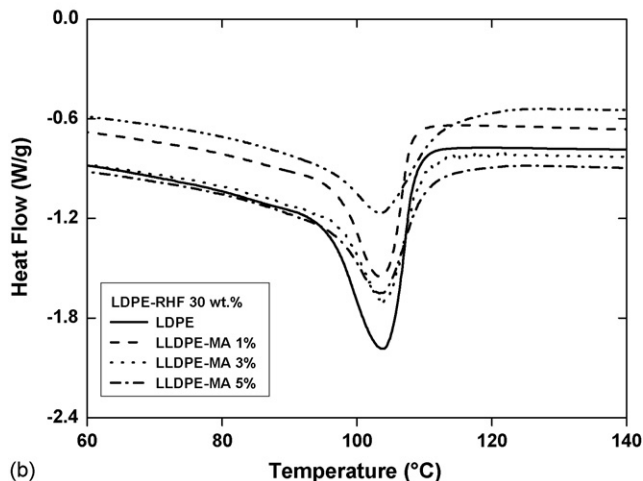
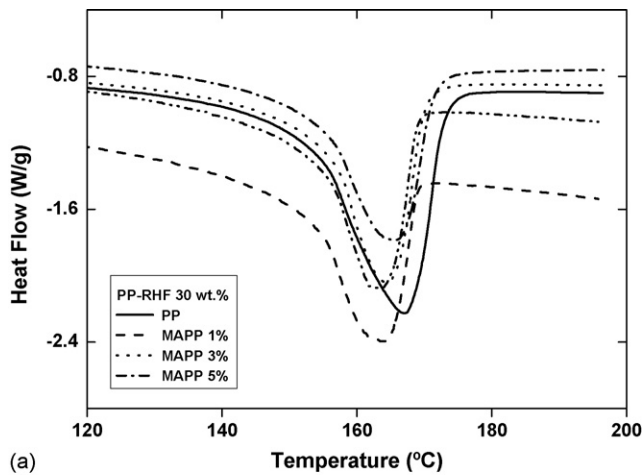


Fig. 11. DSC heating curves of (a) RHF-filled PP and (b) LDPE composites at different MAPP and MAPE (LLDPE-MA) contents.

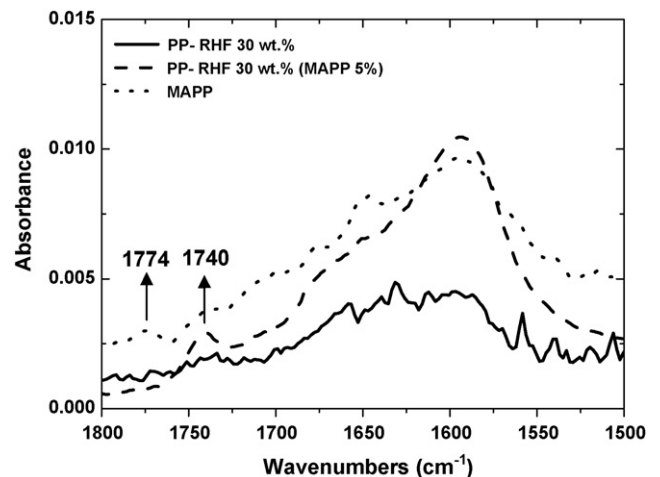


Fig. 12. FTIR-ATR spectra of MAPP, MAPP-treated and non-treated composites.

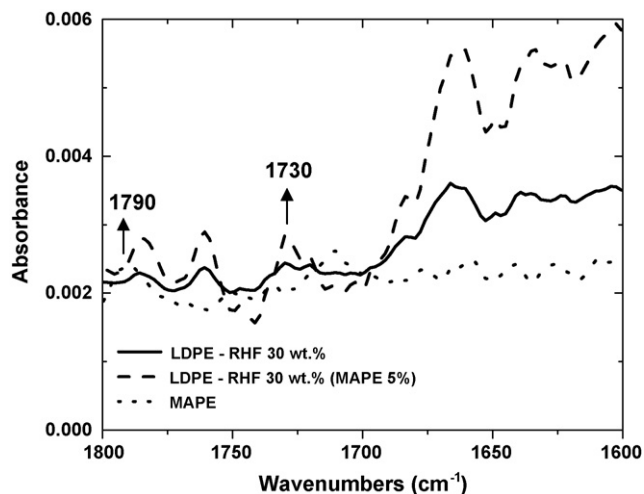


Fig. 13. FTIR-ATR spectra of MAPE (HDPE-MA), MAPE-treated and non-treated composites.

hydroxyl groups and the resultant increased stretching vibration of the carbonyl groups ($C=O$) such as at 1740 cm^{-1} (MAPP) and 1730 cm^{-1} (MAPE) [6,8].

4. Conclusions

The thermal stability, degradation temperature and DTG_{\max} degradation temperature of MAPP- and MAPE-treated composites were slightly higher than those of non-treated composites and were slightly increased with increasing MAPP and MAPE content up to 5%. However, the thermal stability and degradation temperature of the two different base resin types of MAPE-treated composites were not significantly changed. With the incorporation of RHF in PP and LDPE, the E' of PP and LDPE was significantly increased at higher temperature. With increasing MAPP and MAPE content, the E' of composites was slightly increased. The stiffness of the composites was not significantly by the two different base resins. With increasing compatibilizing agent content, $\tan \delta_{\max}$ peak temperature and E''_{\max} peak temperature (β relaxation) of the composites were slightly shifted to a higher temperature while the $\tan \delta$ values of MAPP-treated composites were lower than those of non-treated composites over the complete temperature range due to the decreased energy dissipation. The T_m of the composites was not significantly changed by the addition of MAPP and MAPE. However, the T_g and X_c of the compatibilizing agent-treated composites were slightly increased due to the coupling effect of MAPP and MAPE. The X_c value of the composites with added HDPE-MA was slightly higher than that with added LLDPE-MA. This improvement in

thermal stability and properties could be attributed to improved interfacial adhesion and compatibility between the RHF and matrix due to the treatment of compatibilizing agent. Based on our experimental results, we suggest that the proper method of enhanced interfacial adhesion of composites with LDPE matrix polymer is treatment with HDPE-MA as compatibilizing agent and that the best MAPP and MAPE content is 5%.

Acknowledgement

This work was supported by the Brain Korea 21 project.

References

- [1] P.W. Balasuriya, L. Ye, Y.W. Mai, J. Wu, J. Appl. Polym. Sci. 83 (2002) 2505.
- [2] H. Demir, U. Atikler, D. Balkose, F. Tihminlioglu, Compos. Part A 37 (2006) 447.
- [3] H.S. Kim, H.S. Yang, H.J. Kim, B.J. Lee, T.S. Hwang, J. Therm. Anal. Cal. 81 (2005) 299.
- [4] A. Arbelaiz, B. Fernandez, J.A. Ramos, I. Mondragon, Thermochim. Acta 440 (2005) 103.
- [5] J. Son, H.J. Kim, P.W. Lee, J. Appl. Polym. Sci. 82 (2001) 2709.
- [6] V. Tserki, P. Matzinos, S. Kokkou, C. Panayiotou, Compos. Part A 36 (2005) 965.
- [7] D. Harper, M. Wolcott, Compos. Part A 35 (2004) 385.
- [8] S. Mohanty, S.K. Verma, S.K. Nayak, Compos. Sci. Technol. 3/4 (2006) 538.
- [9] X. Yuan, K. Jayaraman, D. Bhattacharyya, Compos. Part A 35 (2004) 1363–1374.
- [10] A. Espert, W. Camacho, S. Karlson, J. Appl. Polym. Sci. 89 (2003) 2353.
- [11] P. Ganan, I. Mondragon, J. Therm. Anal. Cal. 73 (2003) 783.
- [12] M.A. Lopez-Manchaodo, M. Arroyo, Polymer 41 (2000) 7761.
- [13] D. Ray, B.K. Sarkar, S. Das, A.K. Rana, Compos. Sci. Technol. 62 (2002) 911.
- [14] P.V. Joseph, K. Joseph, S. Thomas, C.K.S. Pillai, V.S. Prasad, G. Groeninckx, M. Sarkissova, Compos. Part A 34 (2003) 253.
- [15] L. Averous, C. Fringant, L. Moro, Polymer 42 (2001) 6565.
- [16] H.S. Kim, H.S. Yang, H.J. Kim, B.J. Lee, T.S. Hwang, J. Therm. Anal. Cal. 76 (2004) 299.
- [17] N.E. Marcovich, M.A. Villar, J. Appl. Polym. Sci. 90 (2003) 2775.
- [18] B. Wielage, Th. Lampke, G. Marx, K. Nestler, D. Starke, Thermochim. Acta 337 (1999) 167.
- [19] H. Hatakeyama, N. Tanamachi, H. Matsumura, S. Hirose, T. Hatakeyama, Thermochim. Acta 421 (2005) 155.
- [20] A. Larena, S.J. Ochoa, F. Dominguez, Polym. Degrad. Stab. 91 (2006) 940.
- [21] C.R. Kumar, I. Fuhrmann, J. Karger-Kocsis, Polym. Degrad. Stab. 76 (2005) 137.
- [22] A.G. Pedroso, D.S. Rosa, Carbohydrate Polym. 59 (2005) 1.
- [23] T. Hatakeyama, F.X. Quinn, Thermal Analysis, John Wiley & Sons Ltd., 1999, 131 pp.
- [24] M. Sclavons, P. Franquinet, V. Carlier, G. Verfaillie, I. Fallais, R. Legras, M. Laurent, F.C. Thyron, Polymer 41 (2000) 1989.
- [25] J.G. Martinez, R. Benavides, C. Guerrero, B.E. Reyes, Polym. Degrad. Stab. 86 (2004) 129.